



THE COLLEGE OF AERONAUTICS
CRANFIELD

The Stresses Around Some Unreinforced
Cutouts Under Various Loading Conditions

- by -

D. S. Houghton, M.Sc.(Eng.),
A.M.I. Mech.E., A.F.R.Ae.S.

and

A. Rothwell, B.Sc.(Eng.), M.S., D.C.Ae.

SUMMARY

A number of experimental results are given for unreinforced circular, elliptical and square cut-outs with rounded corners, under a variety of loading conditions. These results are then compared with the infinite flat plate solution, using the complex stress function and the method of conformal transformation.

It is generally considered sufficiently accurate for a plane stress solution to be applied to problems of cut-outs in cylindrical shells, provided that the cut-out dimensions are small compared with the radius of curvature of the shell. In order to investigate this effect of shell curvature, a number of experiments were carried out on cut-outs in two pressurised cylinders, and to obtain a wider range of loading conditions, a further series of experiments was conducted using a plane loading frame.

Two aluminium alloy cylinders, of 44 in. and 60 in. diameter, were pressurised using air, and the stress conditions around the cut-outs examined using electrical resistance strain gauge techniques.

The plane loading frame enabled any combination of bi-axial tension and shear to be applied to a plane sheet containing the cut-out under examination. In this way the effects of body forces, which might arise in such applications as aircraft and nuclear reactors, could be simulated.

The experimental results which are given generally show a close agreement with the theoretical plane stress solution.

CONTENTS

	<u>Page</u>
Summary	
Notation	
1. Introduction	1
2. Experimental Work	2
3. Theory	4
4. Discussion of Results	9
5. Conclusions	11
6. References	12
Appendix 1. - The method of evaluating the function $\phi(\zeta)$ and the edge stress distribution is shown for an elliptical and a square cut-out in a plane sheet subjected to 2:1 bi-axial tension	14
Figures	

NOTATION

ρ, θ	polar co-ordinates
U	Airy stress function
σ_ρ	radial stress
σ_θ	tangential stress
$\tau_{\rho\theta}$	shear stress
z, ζ	complex variables
ϕ, χ, ψ	complex stress functions
Φ, Ψ	derivatives of complex stress functions
C_n	coefficients in transformation function
σ	complex co-ordinate on the unit circle
$\omega(\zeta)$	transformation function
R	scale factor in transformation function
Γ_1, Γ_2	constants depending upon stresses at infinity
N_1, N_2	principal stresses at infinity
α	direction of principal stress
a_n, b_n	coefficients in series for complex stress functions
Q_c	critical stress combination
λ	stress concentration factor
m	parameter for eccentricity of ellipse
a	semi-major axis of ellipse, or semi-width of square
b	semi-minor axis of ellipse
k	eccentricity of ellipse
β	angle in plane of ellipse or square
r	corner radius of approximate square

1. Introduction

In the design of most shell structures, cut-outs have to be provided for access doors and windows, or to accommodate some intersecting structure. It is well known that their presence causes perturbations in the original stress system, so that in the region of the cut-out the local stress level in the shell may be increased many times. These stress concentrations can of course be considerably reduced, and in some cases entirely eliminated by the use of a suitably chosen shape of cut-out, and by the use of a suitable reinforcing member around the edge. It is the analysis of these cut-outs that constitutes one of the major problems in the design of shell structures.

In the cabin structure of a pressurised aircraft, a long fatigue life must be achieved for minimum structural weight, and the effect of any stress concentrations which may arise in the doors and windows must be closely examined. A similar situation exists in nuclear reactor design, where the true stress conditions at all points in the structure must be accurately determined.

The factors which influence the magnitude of these stress concentrations are the shape of the cut-out and the dimensions of the reinforcement. The geometry of the shell itself is generally of only secondary importance, provided that the size of the cut-out is small compared with the radius of curvature of the shell. If this condition is fulfilled, the coupling between the radial displacement and the stresses in the middle plane of the shell is small, so that the problem may be reduced to that of a cut-out in an infinite plane sheet, which is subjected to the appropriate stress conditions at infinity. In all of the recent theoretical investigations this assumption is made, and according to Gurney¹ is justified for the case of a cut-out in a circular cylinder provided that the ratio of cylinder diameter to cut-out diameter is not less than 4:1.

More recently, Mansfield², Hicks³, and Wittrick⁴ have made similar assumptions and have developed the use of both real stress functions and complex variable methods to predict the stress concentration around unreinforced and reinforced cut-outs of various shapes.

Unfortunately little experimental evidence has been recorded in the literature to support the use of the flat plate theory, and the experimental work which is available is confined to circular cut-outs.

The work which was carried out by Richards⁵ on Xylonite model cylinders suggested that the flat plate theory is inadequate to define the complete stress distribution, since significant bending effects were observed. However Ref. 6 obtained quite a good correlation between a number of photoelastic results, which were obtained on cylinders, and the flat plate theory.

The only theoretical work known to the authors which includes the effect of shell curvature is by Lurie⁷, and this is restricted to small unreinforced circular cut-outs. A closer examination of these papers suggests that for the unreinforced cut-out this discrepancy is not unreasonable, since much depends upon whether the transverse loading across the cut-out is allowed to be reacted at the boundary. The flat plate theory when applied to unreinforced cut-outs does not make allowance for the effect of out of plane forces. For the reinforced cut-out however, it is generally considered that provided the cut-out is neutral, or nearly so, and that the shear distribution around the boundary is in a prescribed manner, then a close agreement should result with the flat plate theory.

In the following paper, a number of experimental results are given for circular, elliptical and square unreinforced cut-outs. Some of the initial experiments were carried out on cylinders which were pressurised using air. These were used to confirm the use of the flat plate theory, and further experiments were subsequently carried out which made use of a plane loading frame. This had the advantage that loading other than pressure loading could be more easily examined.

The analytical work which is presented makes use of the complex stress function and conformal transformation technique of Muskhelishvili⁸ which has been used previously by Wittrick^{9,10} and by the authors^{11,12}.

2. Experimental Work

In order to investigate the validity of the theoretical work, a number of experimental investigations have been undertaken.

Two cylinders were used for the initial experiments, and these measured 44 in. and 60 in. in diameter and were constructed from 18 s.w.g. (0.048 in.) L.72 aluminium alloy sheet. The cylinders were pressurised by using air which was controlled to give a nominal hoop stress of the order of 10,000 lb/in², and were mounted on a specially designed trolley which enabled a free longitudinal expansion of the

cylinder under test to take place (Fig. 14). Investigations were carried out on circular, elliptical and square cut-outs with rounded corners in these cylinders, having dimensions ranging from 6 in. to 10 in.

The air pressure was contained by using a plate which was rolled to the contour of the cylinder and shaped so as to fit accurately into the cut-out (Fig. 15). This was supported by an external structure in such a way that the transverse pressure loading was not reacted at the boundary of the cut-out. This procedure eliminated the substantial bending stresses which would otherwise result, and which for these unreinforced cut-outs would be inconsistent with the flat plate solution. These experiments enabled the effects of shell curvature on the 'in plane' stresses to be examined separately.

Strain gauge readings were taken using Tinsley 6H and 6K electrical resistance strain gauges, in conjunction with a Savage and Parsons recorder. Typical strain gauge positions are shown in Fig. 19.

These preliminary experiments gave a good agreement with the theoretically predicted stress concentration factors using the flat plate theory. This suggested that for the range of cut-outs under examination, any effects of shell curvature on the stress concentration factor were small and that the use of the flat plate theory was justified.

In view of this, and because of the considerable experimental difficulties arising, it was decided to conduct a more ambitious series of experiments using a plane loading frame (Figs. 11, 12). This loading frame enabled bi-axial stress ratios other than the 2:1 biaxial pressure stresses to be studied, and in addition, cut-outs which are subjected to both shear and direct loading could be examined.

The aluminium alloy panels which were used in the plane loading frame were 28 in. square and were made from 16 s.w.g. (.064 in.) L.72 aluminium alloy sheet. Tinsley 6H and 6K electrical resistance strain gauges were again used with the Savage and Parsons recorder. It was found that provided the maximum panel cut-out dimension did not exceed 5 in., any panel boundary effects were negligible, and in this way reasonable comparison could be obtained with the infinite flat plate theory.

The stress concentrations around circular, elliptical and square cut-outs with rounded corners were investigated in the plane loading frame.

The panel was loaded through heavy edge members by means of a linkage system, which was arranged so that if required the effects of direct stress combined with shear stress could be examined (Fig. 13). The loads were produced by two 3000 lb. turnbuckles used in conjunction with calibrated dynamometers. While tensile loading gave edge stresses of up to 1000 lb/in², the shear loading was restricted by panel buckling considerations to 700 lb/in². The strain gauge locations are shown in Figs. 16, 17, 18. The gauges in the region of the cut-out were Tinsley 6H, and the backing paper was trimmed so that strain measurements could be obtained as close as possible to the edge. It was found that measurement of the tangential stress could effectively be made at a distance of 0.1 in. from the edge of the cut-out.

3. Theory

The stresses in the region of circular and elliptic cut-outs in an infinite plane sheet, have been obtained by Inglis¹³ using the real stress function with an elliptical co-ordinate system. This method has been developed by Wells¹⁴ and Hicks³ for certain other cut-out problems.

For other shapes of cut-out, for example square and triangular cut-outs with rounded corners, the method of conformal transformation which has been developed by Muskhelishvili⁸ and used extensively by Savin^{15,16} can be employed. This method can be used for the solution of an unreinforced cut-out of any shape provided that the transformation function can be expressed as a simple polynomial function.

The method and notation of Muskhelishvili have been followed closely here.

The stress components in an elastic plane stress system may be expressed in terms of a single real stress function (the Airy stress function)

$$U(\rho, \theta),$$

satisfying, in the absence of body forces, the biharmonic equation

$$\nabla^4 U = 0,$$

where

$$\nabla^2 = \frac{\partial^2}{\partial \rho^2} + \frac{1}{\rho} \cdot \frac{\partial}{\partial \rho} + \frac{1}{\rho^2} \cdot \frac{\partial^2}{\partial \theta^2}.$$

The stress components in the plane, referred to a polar co-ordinate system (ρ, θ) , are given by

$$\sigma_{\rho} = \frac{1}{\rho} \cdot \frac{\partial U}{\partial \rho} + \frac{1}{\rho^2} \cdot \frac{\partial^2 U}{\partial \theta^2} ,$$

$$\sigma_{\theta} = \frac{\partial^2 U}{\partial \rho^2} ,$$

and

$$\tau_{\rho\theta} = - \frac{\partial}{\partial \rho} \left(\frac{1}{\rho} \cdot \frac{\partial U}{\partial \theta} \right) .$$

Using the complex variable

$$z = \rho e^{i\theta}$$

the biharmonic equation becomes

$$\frac{\partial^4 U}{\partial z^2 \partial \bar{z}^2} = 0 ,$$

and the real stress function may be expressed in complex form, in terms of the two complex functions,

$$\phi(z) \text{ and } \chi(z) ,$$

by

$$2U = \bar{z} \phi(z) + z \overline{\phi(z)} + \chi(z) + \overline{\chi(z)} ,$$

where a bar denotes the complex conjugate.

If $\phi(z)$ and $\chi(z)$ are holomorphic functions, every expression of this form represents a biharmonic function.

The stress components in the polar co-ordinate system are then given by

$$\sigma_{\rho} + \sigma_{\theta} = 2 [\phi(z) + \overline{\phi(z)}]$$

and

$$\sigma_{\theta} - \sigma_{\rho} + 2i\tau_{\rho\theta} = 2 [\bar{z} \phi'(z) + \psi(z)] e^{2i\theta} ,$$

where

$$\psi(z) = \chi'(z) ,$$

$$\bar{\psi}(z) = \phi'(z) ,$$

$$\Psi(z) = \psi'(z) ,$$

and the prime denotes differentiation with respect to z .

The region Σ in the ζ -plane may be transformed into the region S in the z -plane by a conformal transformation function

$$z = \omega(\zeta),$$

where $\omega(\zeta)$ is a single valued analytic function.

Transformation functions of the form

$$\omega(\zeta) = R \left[\zeta + \frac{C_1}{\zeta} + \frac{C_2}{\zeta^2} + \dots \right]$$

have been obtained, which transform an infinite plane sheet containing an elliptic or approximate square cut-out in the z -plane into the region outside the unit circle

$$\sigma = e^{i\theta}$$

in the ζ -plane. Similar transformation functions may be obtained for cut-outs of other shapes⁹.

If the functions previously written

$$\phi(z) \quad \psi(z) \quad \Phi(z) \quad \Psi(z)$$

are now denoted by

$$\phi_*(z) \quad \psi_*(z) \quad \Phi_*(z) \quad \Psi_*(z)$$

then in the new notation

$$\phi(\zeta) = \phi_*(z) = \phi_*[\omega(\zeta)],$$

$$\psi(\zeta) = \psi_*(z) = \psi_*[\omega(\zeta)],$$

and

$$\Phi(\zeta) = \frac{\phi'(\zeta)}{\omega'(\zeta)},$$

$$\Psi(\zeta) = \frac{\psi'(\zeta)}{\omega'(\zeta)}.$$

In the transformed plane the stress components, denoted by σ_r , σ_θ and $\tau_{r\theta}$ in the curvilinear co-ordinate system corresponding to the polar co-ordinate system in the ζ -plane, are given by

$$\sigma_{\rho} + \sigma_{\theta} = 2 \left[\Phi(\zeta) + \overline{\Phi(\zeta)} \right] = 4 \operatorname{Re.} \left[\Phi(\zeta) \right],$$

and

$$\sigma_{\theta} - \sigma_{\rho} + 2i\tau_{\rho\theta} = \frac{2\zeta^2}{\rho^2 \overline{\omega'(\zeta)}} \left[\overline{\omega(\zeta)} \cdot \Phi'(\zeta) + \omega'(\zeta) \Psi(\zeta) \right],$$

where Re denotes the real part.

At the edge of an unreinforced cut-out

$$\sigma_{\rho} = \tau_{\rho\theta} = 0,$$

so that to find the stress at the edge of the cut-out the function $\Psi(\zeta)$ is not required, and the problem is reduced to that of finding the function $\Phi(\zeta)$ satisfying the boundary conditions of the problem.

The expression for the edge stress then becomes

$$\sigma_{\theta} = 4 \operatorname{Re.} \left[\Phi(\zeta) \right].$$

The boundary condition on the edge of the cut-out (since there are no external forces applied to the edge of the cut-out) may be written

$$\phi(\sigma) + \frac{\omega(\sigma)}{\overline{\omega'(\sigma)}} \cdot \overline{\phi'(\sigma)} + \overline{\psi(\sigma)} = 0,$$

where $\sigma = e^{i\theta}$ on the unit circle.

The complex stress functions $\phi(\zeta)$ and $\psi(\zeta)$ may be expressed

$$\phi(\zeta) = \phi_0(\zeta) + \phi_1(\zeta)$$

and

$$\psi(\zeta) = \psi_0(\zeta) + \psi_1(\zeta),$$

where the functions $\phi_1(\zeta)$ and $\psi_1(\zeta)$ represent the state of stress at infinity, and $\phi_0(\zeta)$, $\psi_0(\zeta)$ are the perturbation functions due to the presence of the cut-out.

Hence $\phi_1(\zeta)$ and $\psi_1(\zeta)$ are given by

$$\phi_1(\zeta) = R \Gamma_1 \zeta$$

and

$$\psi_1(\zeta) = R \Gamma_2 \zeta$$

where

$$\Gamma_1 = \frac{1}{4} (N_1 + N_2) ,$$

$$\Gamma_2 = -\frac{1}{2} (N_1 - N_2) e^{-2i\alpha} ,$$

and N_1, N_2 are the values of the principal stresses at infinity, α is the angle made by the direction of N_1 with the axis $\theta = 0$, and R is the scale factor in the transformation function.

The functions $\phi_0(\zeta)$ and $\psi_0(\zeta)$, which are homomorphic outside the unit circle including the point at infinity, may be expanded into series of the form

$$\phi_0(\zeta) = \frac{a_1}{\zeta} + \frac{a_2}{\zeta^2} + \frac{a_3}{\zeta^3} + \dots = \sum_{n=1}^{\infty} a_n \zeta^{-n}$$

and

$$\psi_0(\zeta) = \frac{b_1}{\zeta} + \frac{b_2}{\zeta^2} + \frac{b_3}{\zeta^3} + \dots = \sum_{n=1}^{\infty} b_n \zeta^{-n} .$$

On the unit circle

$$\zeta = \sigma = e^{i\theta} ,$$

and the term

$$\frac{\omega(\sigma)}{\omega'(\sigma)}$$

may be expanded into a series of ascending powers of σ .

By substituting this, together with the series expansions for $\phi(\zeta)$ and $\psi(\zeta)$, into the boundary condition on the edge of the cut-out the coefficients a_n may be determined by equating coefficients of powers of σ in the boundary condition.

Since the function $\phi(\zeta)$ alone is sufficient to obtain the stress at the edge of the cut-out, it is not necessary to determine the coefficients b_n .

In the appendix, the function $\phi(\zeta)$ and the stress distribution σ_θ at the edge of the cut-out have been evaluated for two particular cases of an elliptical and a square cut-out, to illustrate the method of solution.

The stress concentration factor λ is based on the 'critical stress combination'¹⁷ which is given by

$$Q = \sigma_r^2 + \sigma_\theta^2 - \sigma_r \sigma_\theta + 3\tau_{r\theta}^2,$$

and the stress concentration factor is then given by

$$\lambda = \sqrt{\frac{Q}{[Q]_\infty}}.$$

4. Discussion of Results

The stress concentration factors obtained from the infinite flat plate theory, for unreinforced circular and elliptical cut-outs under various systems of bi-axial tension and pure shear, are shown in Figs. 1, 3 and 4.

For the circular and elliptical cut-outs under bi-axial tension, the maximum stress concentration occurs at the edge of the cut-out, where the tangent is in the direction of the maximum applied stress. The maximum value of λ is dependent on the ratio $n:1$ of the applied stresses. An increase in n above 2 leads to a relatively small increase in the stress concentration factor. For a circular cut-out subjected to 2:1 bi-axial tensions, the stress concentration factor is approximately 3.

For an elliptical cut-out the stress concentration factor also depends on the eccentricity b/a of the ellipse, and a smaller value of λ is produced when the major axis of the ellipse is in the direction of the maximum applied stress. There is an optimum value of b/a for the minimum stress concentration, which is dependent on the ratio of the applied stresses.

Under pure shear, the stress concentration factor for an elliptical cut-out is again dependent on the eccentricity b/a and the direction of the axes. For a circular cut-out under pure shear a symmetrical stress distribution is obtained and the maximum value of λ is approximately 2.25.

The theoretical stress concentration factors for unreinforced square cut-outs having various corner radii, and under various systems of bi-axial tension and pure shear, are shown in Figs. 7 and 8. By retaining the first few terms only in the transformation function for the square, a limited number of different corner radii may be obtained. The profiles of the approximate squares obtained by retaining two and three terms only in the transformation function are shown in Fig. 6.

By suitable modification of the coefficients, Wittrick⁹ has obtained a more general transformation function for a square having any corner radius. This method may also be applied to triangular cut-outs and other shapes.

For a square cut-out the maximum stress concentration, under both bi-axial tension and pure shear, occurs at the corner of the square, and the maximum value of λ is dependent on the corner radius r/a . Very high stress concentrations are obtained when the corner radius is small. Under bi-axial tension, the maximum stress concentration depends on the ratio $n:1$ of the applied stresses, and is actually decreased as the value of n is increased.

The stress concentrations for loading cases other than those shown, may be obtained by superposition of the curves. In this way the effect of biaxial tensions which are not parallel to the axes of symmetry of the cut-out, and the effect of combined tensile and shear loading may be deduced.

A number of preliminary tests were carried out on circular and elliptic cut-outs in the pressure cylinders to investigate the importance of the effect of curvature of the shell. It was deduced from these that, for the range of cut-outs investigated, the effect of curvature was small and could conveniently be neglected. For this reason a large part of the subsequent experimental work was carried out on the plane loading frame.

The experimental results shown in Fig. 10 were obtained on the 60 in. diameter cylinder subjected to internal pressure, and those shown in Figs. 2, 5 and 9 were obtained using the plane loading frame.

In order to examine the strain distribution across the panel in the plane loading frame, some preliminary tests were carried out on an uncut panel (Fig. 12). These results indicated that under tensile loading, the strains along the horizontal and vertical axes were between -12% and -6% of the nominal values. Under shear loading, the strain was approximately constant across the panel width. There was a tendency for the shear stress to peak near the corners, where the strain was 5% higher than the nominal strain.

The qualitative agreement between the experimental and theoretical results is good. The experimental values are generally lower than the theoretical, and this is to be expected since the strain gauge readings are

made at a distance of 0.1 in. from the edge of the cut-out in most cases, owing to the physical dimensions of the strain gauges. Extrapolation of the strain gauge readings could have been carried out in order to eliminate this effect, but the preliminary attempts showed that large errors could occur in the extrapolation owing to rapid changes in strain away from the edge of the cut-out.

In the experiments on the square cut-out, when both the pressure cylinder and the plane loading frame were used, the maximum stress concentration at the corner of the square was difficult to measure, owing to the rapid increase in the stress concentration in this region and the size of the strain gauge.

5. Conclusions

The results are given of a number of tests carried out on unreinforced cut-outs of various shapes in pressurised cylinders and in a plane loading frame.

These results are compared with the theory, and the general agreement is found to be good in most cases.

Having now established the technique, it is hoped to continue with a further programme of experimental work for reinforced cut-outs of various shapes, under a variety of loading conditions.

6. References

1. Gurney, C. Analysis of the stresses in a flat plate with a reinforced circular hole under edge forces.
A.R.C., R & M. 1834, 1938.
2. Mansfield, E.H. Neutral holes in a plane sheet.
A.R.C., R & M. 2815, 1955.
3. Hicks, R. Reinforced elliptical holes in stressed plates.
Journal of the Royal Aeronautical Society, vol.61, 1957, pp 688-693.
4. Wittrick, W.H. Stresses around reinforced elliptical holes, with applications to pressure cabin windows.
Aeronautical Quarterly, vol.10, Nov.1959.
5. Richards, T.H. Stress distribution in pressurised cabins: An experimental study by means of Xylonite models.
A.R.C. 19,360. Strut.1999, 1957.
6. Houghton, D.S. Stress concentrations around cut-outs in a cylinder. (To be published by Royal Aeronautical Society).
7. Lurie, A.I. Statics of thin walled elastic shells.
Cgiz, Moscow. 1947.
8. Muskhelishvili, N.I. Some basic problems of the mathematical theory of elasticity.
Noordhoff, Groningen, Holland, 1953.
9. Wittrick, W.H. Some simple transformation functions for square and triangular holes with rounded corners.
Aeronautical Quarterly, vol.11, May 1960, pp 195-199.

References (Continued)

10. Wittrick, W.H. Analysis of stress concentrations at reinforced holes in infinite sheets. Aeronautical Quarterly, vol.11, Aug.1960.
11. Houghton, D.S. Nuclear reactor containment buildings and pressure vessels. Butterworths, London, 1960, pp 191-220.
12. Hillel, A.,
 Rothwell, A., Unpublished thesis work conducted at
 Arthurs, T.D. the College of Aeronautics, Cranfield.
13. Inglis, C.E. Stresses in a plate due to the presence of cracks and sharp corners. Trans. of the Inst. Naval Arch. vol.55, 1913, p 219.
14. Wells, A.A. On the plane stress distribution in an infinite plane with rim-stiffened elliptical opening. Quarterly Journal of Mechanics and Applied Mathematics, vol.3, 1950, p 23.
15. Savin, G.N. Stress concentrations around holes. Veb. Verlag Technik, Berlin, 1956. (German translation).
16. Godfrey, D.E.R. Report on Savin's 'Stress concentration around holes'. A.R.C.18460, Struct.1895, 1956.
17. Timoshenko, S., Theory of elasticity.
 Goodier, J.N. McGraw-Hill, New York, 1951.

APPENDIX 1

The method of evaluating the function $\phi(\zeta)$ and the edge stress distribution is shown for an elliptical and a square cut-out in a plane sheet subjected to 2:1 bi-axial tension.

(a) Elliptical Cut-out (Fig. 20a)

The region outside an ellipse in the z -plane may be transformed on to the region outside the unit circle in the ζ -plane by the transformation function

$$z = \omega(\zeta) = R\left(\zeta + \frac{m}{\zeta}\right), \quad \begin{matrix} R > 0 \\ 0 \leq m < 1 \end{matrix}$$

The circle

$$|\zeta| = 1$$

corresponds to an ellipse with centre at the origin and semi-axes

$$a = R(1 + m),$$

$$b = R(1 - m),$$

and therefore

$$m = \frac{1 - k}{1 + k},$$

where $k = \frac{b}{a}.$

Differentiation of the transformation function gives

$$\omega'(\zeta) = R\left(1 - \frac{m}{\zeta^2}\right).$$

On the unit circle

$$\zeta = \sigma = e^{i\theta},$$

and

$$\frac{1}{\zeta} = \frac{1}{\sigma}.$$

Therefore

$$\frac{\omega(\sigma)}{\omega'(\sigma)} = \frac{\sigma + \frac{m}{\sigma}}{1 - m\sigma^2},$$

or expanding this equation as an ascending power series

$$\frac{\omega(\sigma)}{\omega'(\sigma)} = \frac{m}{\sigma} + (1 + m^2)\sigma + m(1 + m^2)\sigma^3 + \dots$$

The complex stress functions may be written

$$\phi(\zeta) = \phi_0(\zeta) + \phi_1(\zeta),$$

$$\psi(\zeta) = \psi_0(\zeta) + \psi_1(\zeta),$$

and the functions $\phi_1(\zeta)$ and $\psi_1(\zeta)$ are obtained from the conditions at infinity.

In this case

$$N_1 = 2, \quad N_2 = 1,$$

$$\alpha = 0.$$

Therefore

$$\Gamma_1 = \frac{1}{4} (N_1 + N_2) = \frac{3}{4}$$

$$\Gamma_2 = -\frac{1}{2} (N_1 - N_2) e^{-2i\alpha} = -\frac{1}{2},$$

and

$$\phi_1(\zeta) = \frac{3}{4} R\zeta,$$

$$\psi_1(\zeta) = -\frac{1}{2} R\zeta.$$

The perturbation functions may be expanded in the form

$$\phi_0(\zeta) = \sum_{n=1}^{\infty} a_n \zeta^{-n},$$

$$\psi_0(\zeta) = \sum_{n=1}^{\infty} b_n \zeta^{-n},$$

and differentiation gives

$$\phi'_0(\zeta) = \sum_{n=1}^{\infty} -na_n \zeta^{-n-1}.$$

Therefore

$$\overline{\phi'(\sigma)} = - \sum_1^{\infty} \bar{n} a_n \sigma^{n+1} + \frac{3}{4} R$$

and

$$\overline{\psi(\sigma)} = \sum_1^{\infty} \bar{b}_n \sigma^n - \frac{1}{2} \cdot \frac{R}{\sigma}.$$

The boundary condition to be satisfied on the unit circle is

$$\phi(\sigma) + \frac{\omega(\sigma)}{\omega'(\sigma)} \cdot \overline{\phi'(\sigma)} + \overline{\psi(\sigma)} = 0.$$

Substitution in the boundary condition gives

$$\begin{aligned} \frac{3}{4} R \sigma + \sum_1^{\infty} a_n \sigma^{-n} \\ + \left[\frac{m}{\sigma} + (1+m^2)\sigma + m(1+m^2)\sigma^3 + \dots \right] \times \\ \left[\frac{3}{4} R - \sum_1^{\infty} \bar{n} a_n \sigma^{n+1} \right] \\ - \frac{1}{2} \cdot \frac{R}{\sigma} + \sum_1^{\infty} \bar{b}_n \sigma^n \\ = 0. \end{aligned}$$

The coefficients a_n may be obtained from this equation by comparing coefficients of negative powers of σ .

Thus

$$a_1 = \left(\frac{2-3m}{4} \right) R,$$

and all the other coefficients a_n are zero.

It is not necessary to determine the coefficients b_n since the function $\phi(\zeta)$ alone is sufficient to obtain the edge stress distribution.

Therefore

$$\phi(\zeta) = \frac{3}{4} R \zeta + \frac{(2-3m) R}{4 \zeta}.$$



and
$$\phi'(\zeta) = \frac{3}{4} R - \frac{(2-3m)R}{2\zeta^2} .$$

Now
$$\Phi(\zeta) = \frac{\phi'(\zeta)}{\omega'(\zeta)} = \frac{\frac{3}{4}\zeta^2 - \frac{2-3m}{2}}{\zeta^2 - m} ,$$

and the edge stress is given by

$$\sigma_{\theta} = 4 \operatorname{Re} [\Phi(\zeta)] .$$

On the boundary

$$\zeta = \sigma = e^{i\theta} ,$$

and the edge stress is

$$\sigma_{\theta} = \frac{3 - 2 \cos 2\theta - 3m^2 + 2m}{1 - 2m \cos 2\theta + m^2} .$$

Thus an expression is obtained for the stress distribution at the edge of an elliptical cut-out of any eccentricity in a plane sheet subjected to 2:1 bi-axial tension.

It should be noted that the angle θ in the expression for the edge stress refers to the unit circle, and the corresponding angle β on the ellipse is given by

$$\tan \beta = k \tan \theta .$$

In this case, the critical stress combination

$$[Q]_{\infty} = 3 ,$$

and the stress concentration factor is

$$\lambda = \frac{\sigma_{\theta}}{\sqrt{3}} .$$

A circular cut-out may be regarded as a particular case of an elliptical cut-out with $m = 0$, and in this case the edge stress becomes

$$\sigma_{\theta} = 3 - 2 \cos 2\theta .$$

(b) Square Cut-out (Fig. 20b)

The region outside a square in the z -plane may be transformed on to the region outside the unit circle in the ζ -plane by the transformation function

$$z = \omega(\zeta) = R \left(\zeta - \frac{1}{6\zeta^3} + \frac{1}{56\zeta^7} - \frac{1}{176\zeta^{11}} + \frac{1}{384\zeta^{15}} + \dots \right),$$

$$R > 0.$$

By retaining the first few terms only of this expansion, an approximate square with rounded corners is obtained, and by increasing the number of terms the corner radius is reduced.

If the first two terms only are retained in the transformation function

$$\omega(\zeta) = R \left(\zeta - \frac{1}{6\zeta^3} \right),$$

an approximate square is obtained having semi-width

$$a = \frac{5}{6} R,$$

and corner radius

$$r = 0.12a.$$

The exact profile of the approximate square obtained by this transformation is shown in Fig. 6(a).

Differentiation of the transformation function gives

$$\omega'(\zeta) = R \left(1 + \frac{1}{2\zeta^4} \right).$$

On the unit circle

$$\zeta = \sigma = e^{i\theta},$$

and

$$\frac{1}{\zeta} = \frac{1}{\sigma}.$$

Therefore

$$\frac{\omega(\sigma)}{\omega'(\sigma)} = \frac{\sigma - \frac{1}{6\sigma^3}}{1 + \frac{\sigma^4}{2}},$$

or expanding this as an ascending power series

$$\frac{\omega(\sigma)}{\omega'(\sigma)} = -\frac{1}{6\sigma^3} + \frac{13}{12}\sigma - \frac{13}{24}\sigma^5 + \dots$$

As for the elliptical cut-out, the complex stress functions may be expressed by

$$\begin{aligned} \phi(\zeta) &= \sum_{n=1}^{\infty} a_n \zeta^{-n} + \frac{3}{4} R \zeta, \\ \psi(\zeta) &= \sum_{n=1}^{\infty} b_n \zeta^{-n} - \frac{1}{2} R \zeta, \\ \text{and} \\ \overline{\phi'(\sigma)} &= -\sum_{n=1}^{\infty} n \bar{a}_n \sigma^{n+1} + \frac{3}{4} R, \\ \overline{\psi(\sigma)} &= \sum_{n=1}^{\infty} \bar{b}_n \sigma^n - \frac{1}{2} \frac{R}{\sigma}. \end{aligned}$$

By substituting these expressions in the boundary condition

$$\phi(\sigma) + \frac{\omega(\sigma)}{\omega'(\sigma)} \cdot \overline{\phi'(\sigma)} + \overline{\psi(\sigma)} = 0,$$

an equation is obtained to determine the coefficients a_n , as

$$\begin{aligned} \frac{3}{4} R \sigma + \sum_{n=1}^{\infty} a_n \sigma^{-n} &+ \left[-\frac{1}{6\sigma^3} + \frac{13}{12}\sigma - \frac{13}{24}\sigma^5 + \dots \right] \cdot \left[\frac{3}{4} R - \sum_{n=1}^{\infty} n \bar{a}_n \sigma^{n+1} \right] \\ &- \frac{1}{2} \frac{R}{\sigma} + \sum_{n=1}^{\infty} \bar{b}_n \sigma^n = 0. \end{aligned}$$

By comparing coefficients of negative powers of σ in this equation we find

$$a_1 = \frac{3}{7} R ,$$

$$a_3 = \frac{1}{8} R ,$$

and all the other coefficients a_n are zero.

Therefore

$$\phi(\zeta) = \frac{3}{4} R \zeta + \frac{3}{7} \cdot \frac{R}{\zeta} + \frac{1}{8} \cdot \frac{R}{\zeta^3} ,$$

and

$$\phi'(\zeta) = \frac{3}{4} R - \frac{3}{7} \cdot \frac{R}{\zeta^2} - \frac{3}{8} \cdot \frac{R}{\zeta^4} .$$

Now

$$\Phi(\zeta) = \frac{\phi'(\zeta)}{\omega'(\zeta)} = \frac{\frac{3}{4} \cdot \zeta^4 - \frac{3}{7} \cdot \zeta^2 - \frac{3}{8}}{\zeta^4 + \frac{1}{2}} ,$$

and the edge stress is given by

$$\sigma_\theta = 4 \operatorname{Re} [\Phi(\zeta)] .$$

On the boundary

$$\zeta = \sigma = e^{i\theta} ,$$

and the edge stress is

$$\sigma_\theta = \frac{63 - 72 \cos 2\theta}{35 + 28 \cos 4\theta} ,$$

for a square cut-out having corner radius $0.12a$ in a plane sheet subjected to 2:1 bi-axial tension.

Again, the angle θ refers to the unit circle, and the corresponding angle β on the square is given by

$$\tan \beta = \frac{\sin \theta + \frac{1}{6} \sin 3\theta}{\cos \theta - \frac{1}{6} \cos 3\theta} .$$

By retaining more terms in the transformation function, the stress distribution around square cut-outs having certain other corner radii may be obtained.

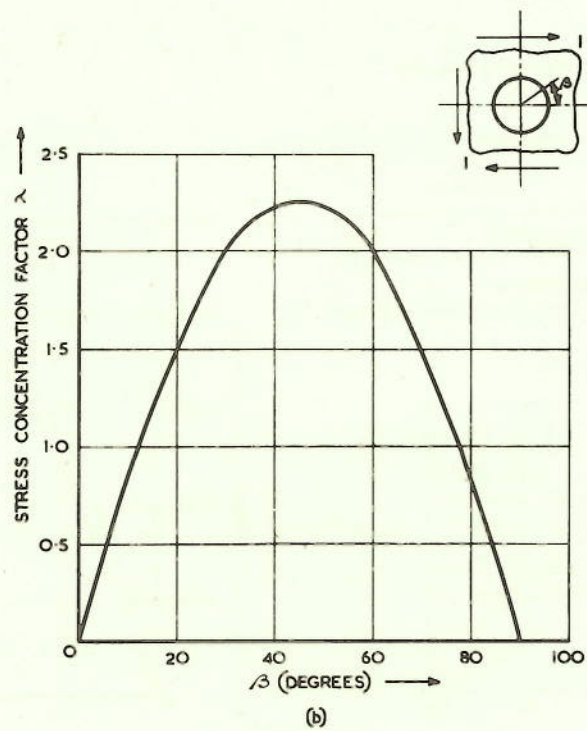
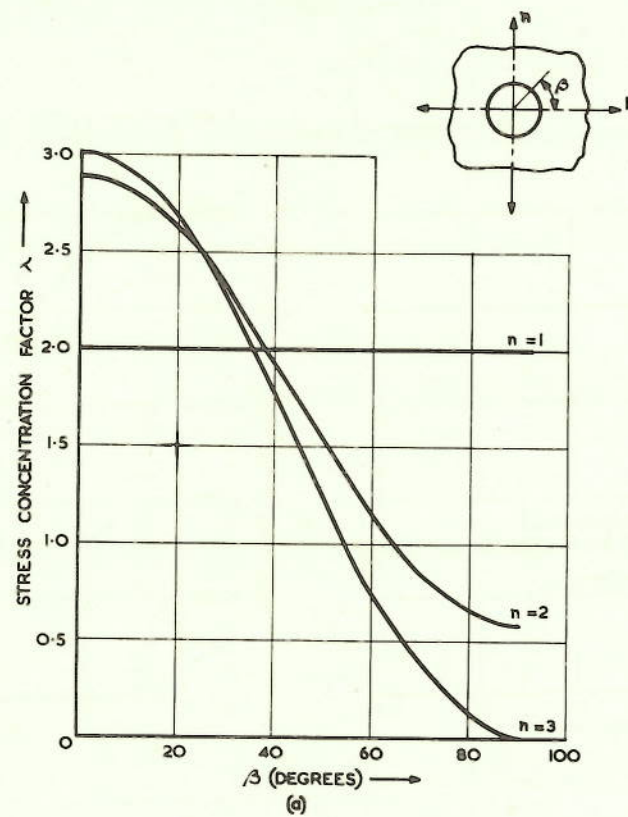


FIG. 1. Circular cut-out: Theoretical stress concentration factor when plate is subjected to biaxial tension or shear

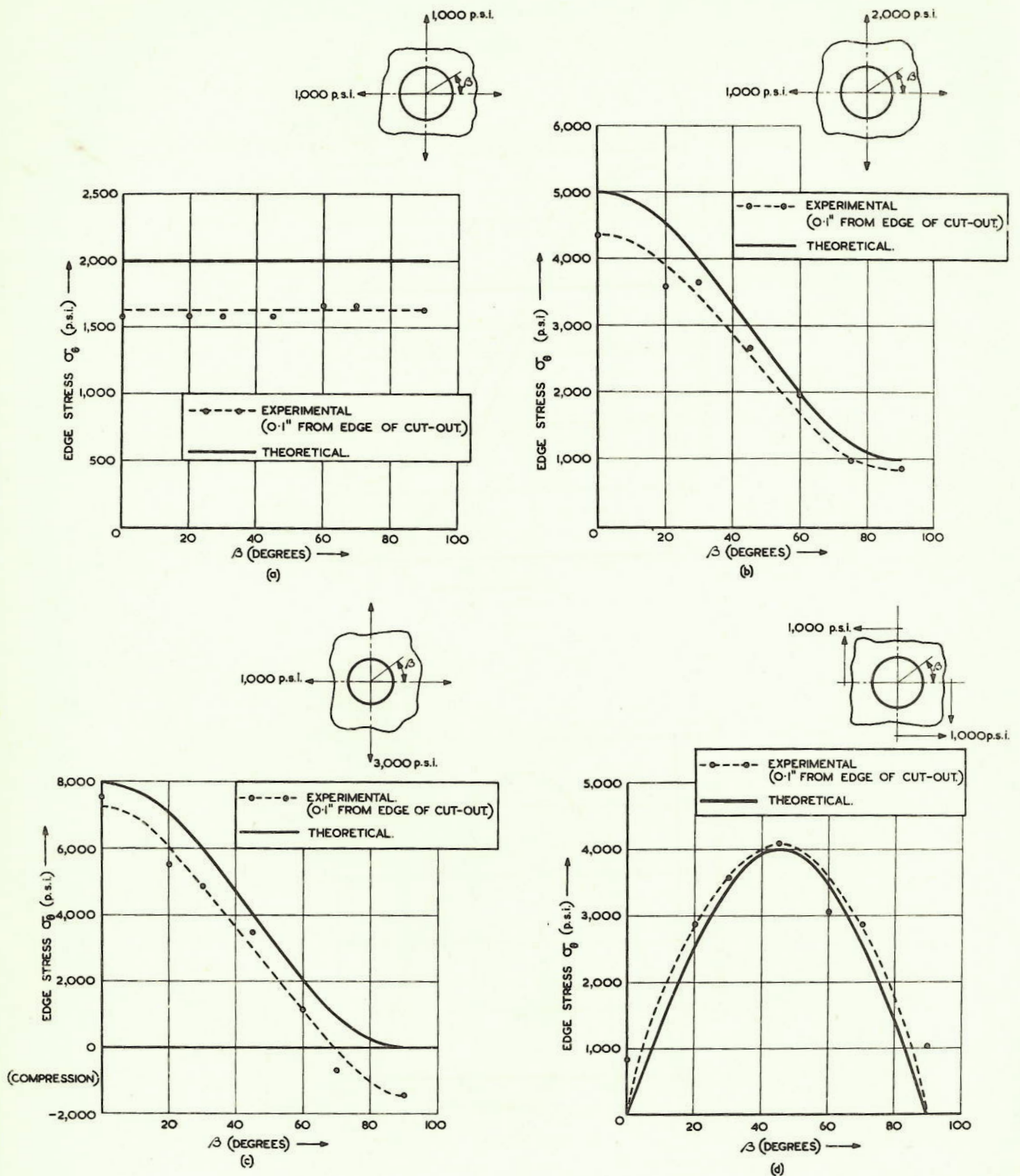


FIG. 2. Circular cut-out: A comparison between experimental and theoretical stress distributions when the plate is subjected to biaxial tension or shear.

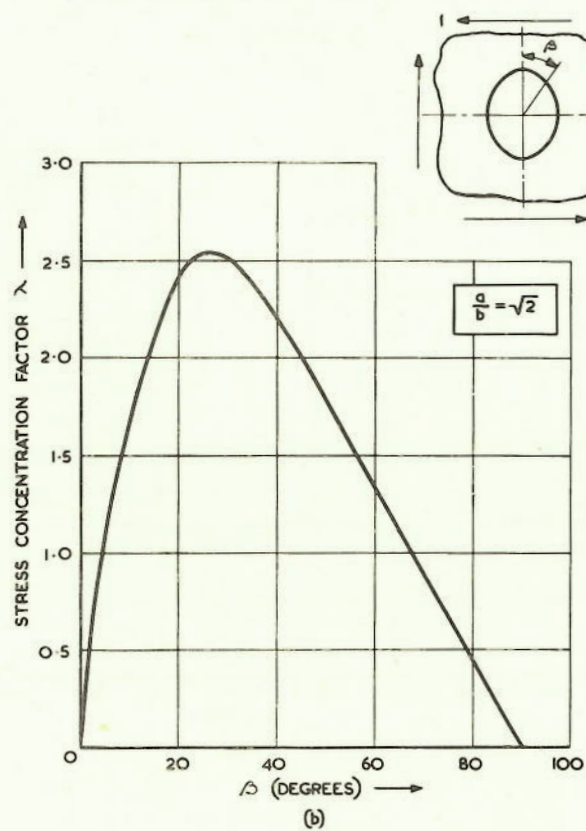
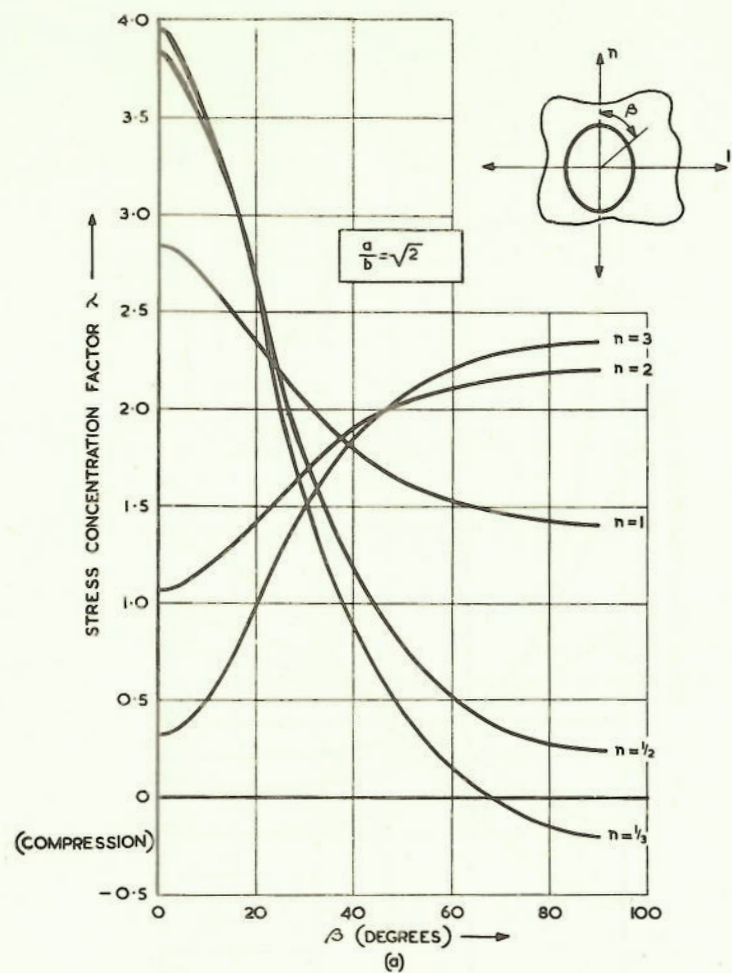


FIG. 3. $\sqrt{2}:1$ Elliptical cut-out: Theoretical stress concentration factor when plate is subjected to biaxial tension or shear

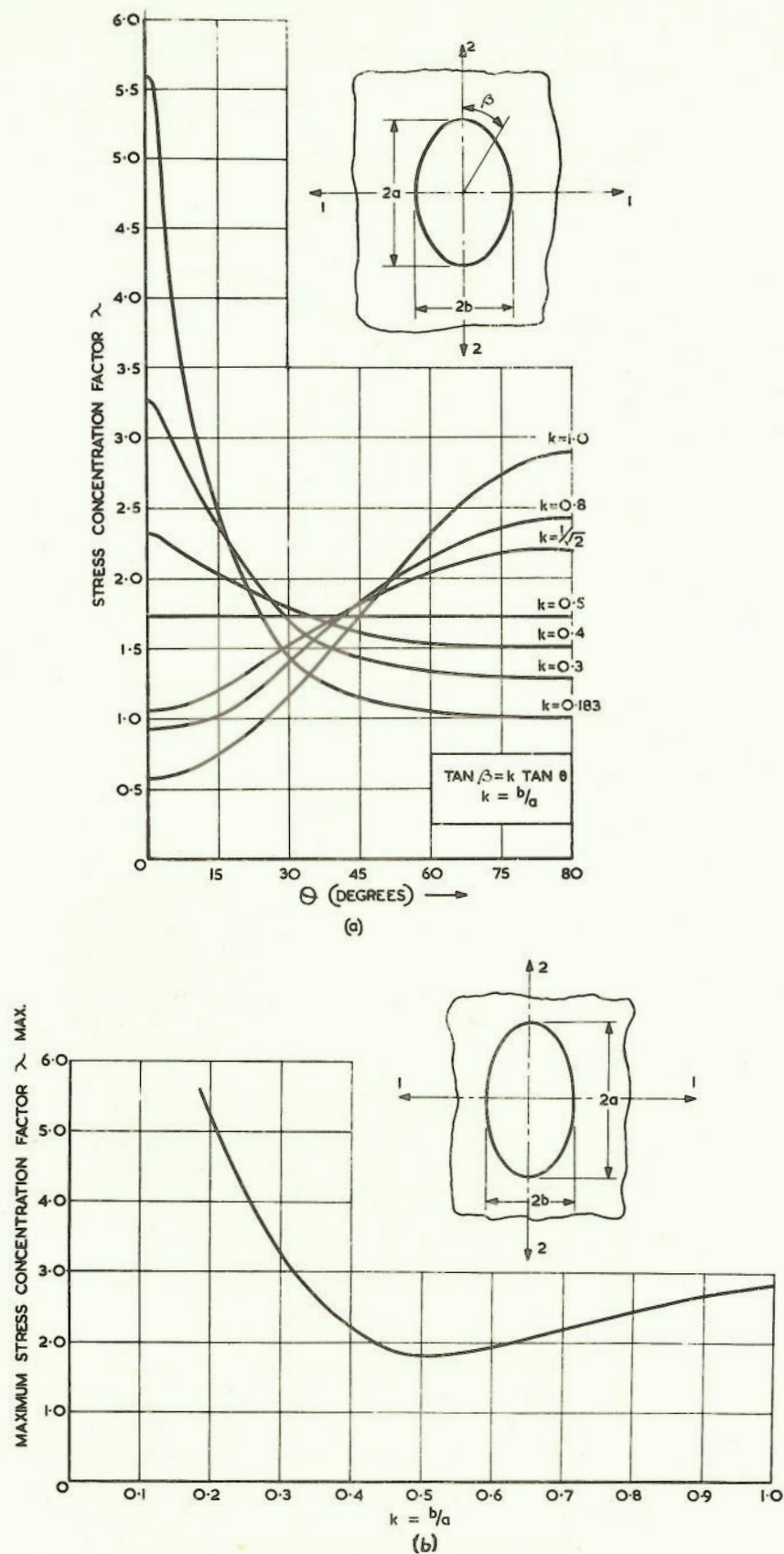


FIG. 4. Elliptical cut-out: Theoretical stress concentration factor for various values of eccentricity when plate is subjected to 2:1 biaxial tension

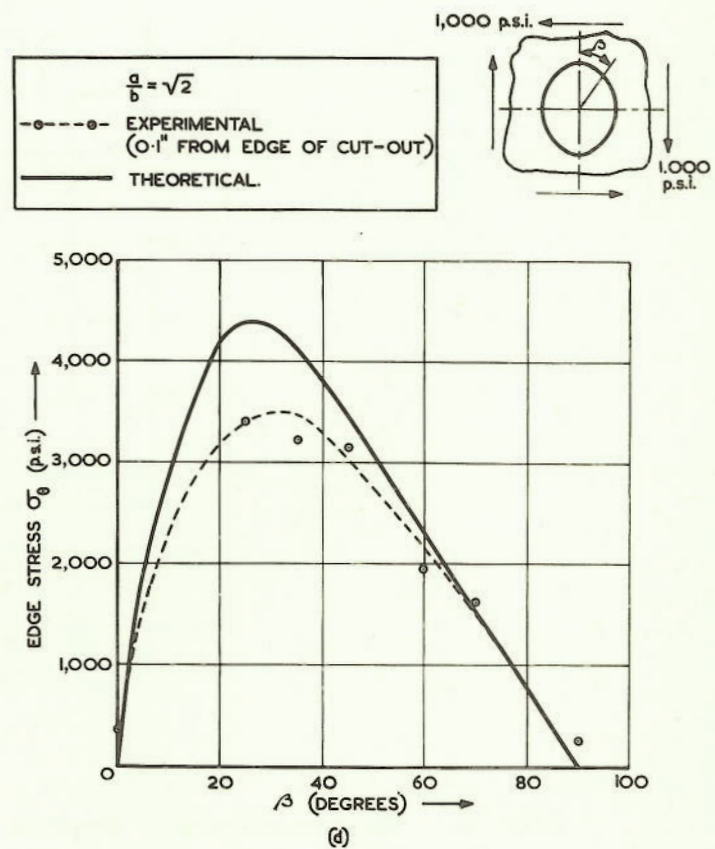
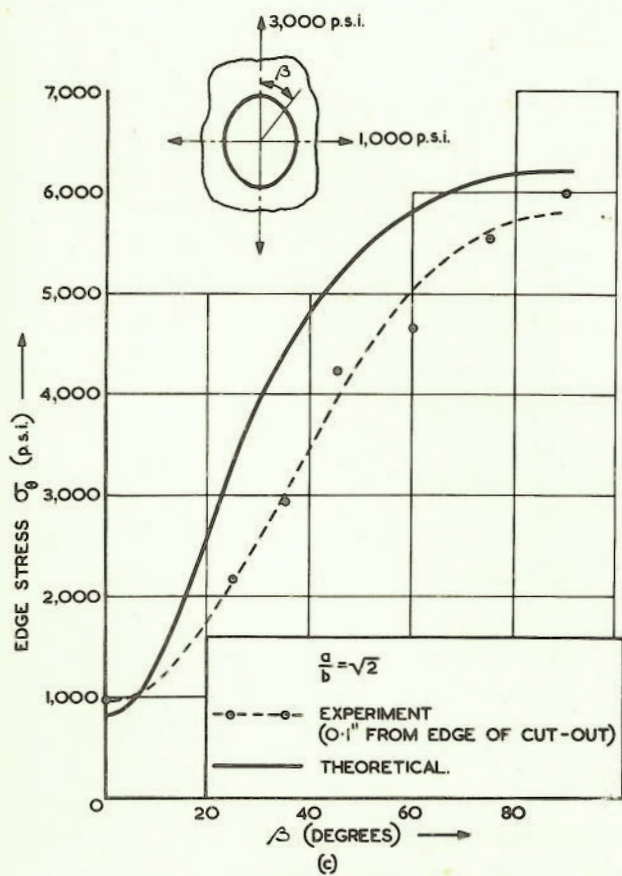
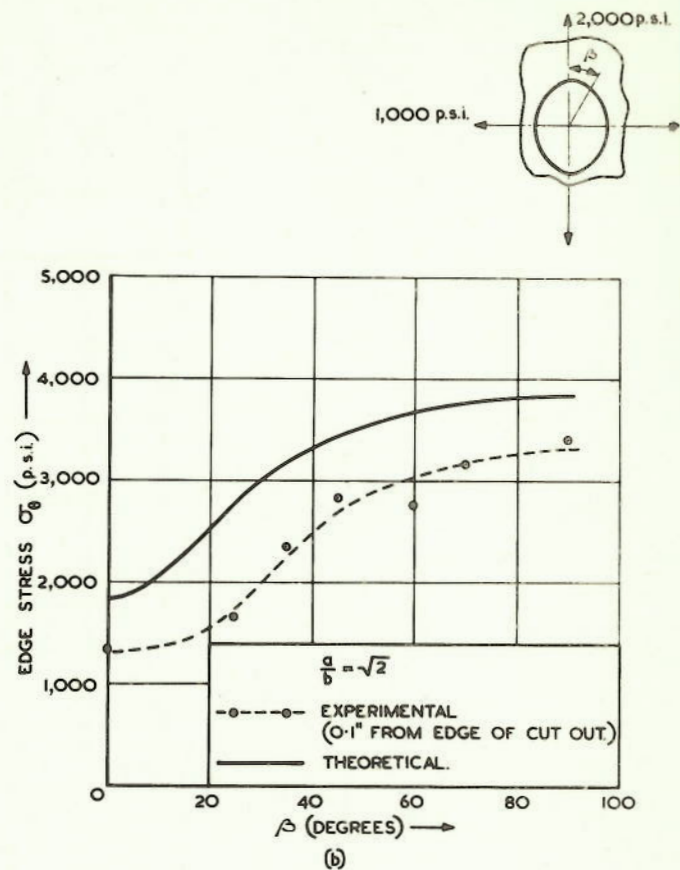
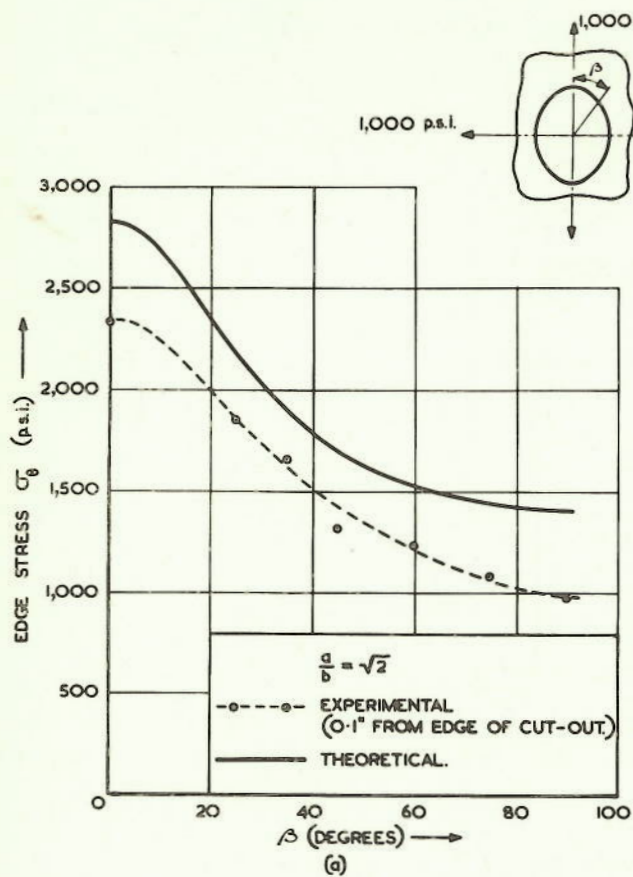
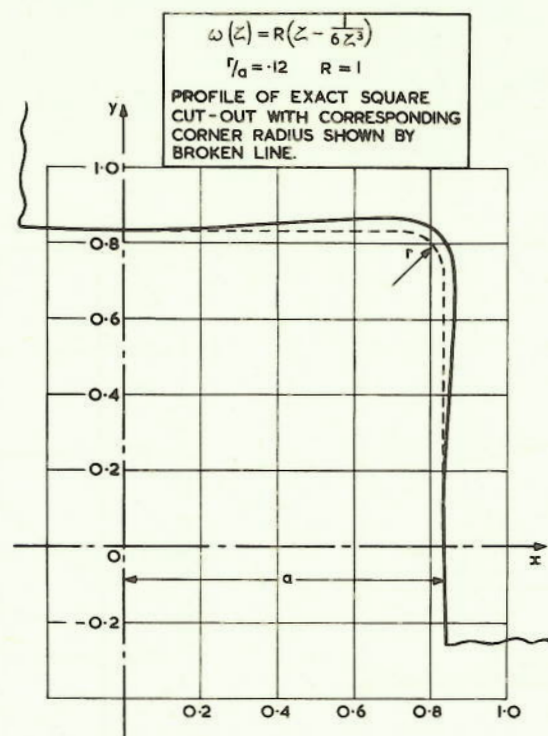
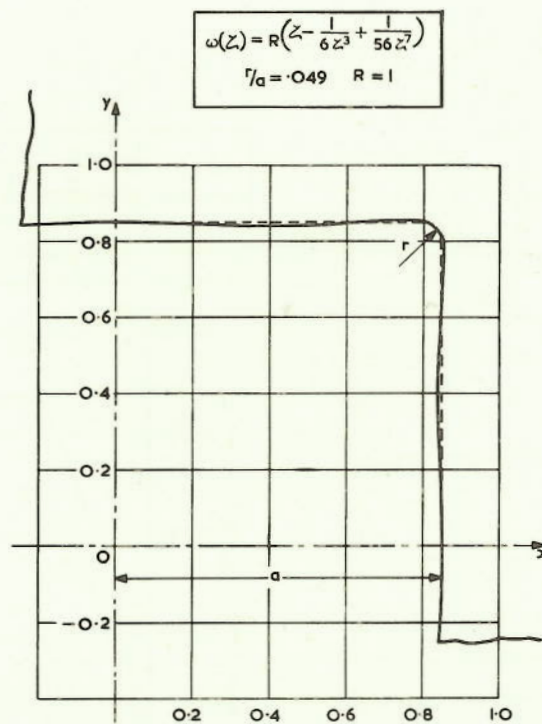


FIG. 5. $\sqrt{2}:1$ Elliptical cut-out: A comparison between experimental and theoretical stress distributions when the plate is subjected to biaxial tension or shear



(a)



(b)

FIG. 6. Square cut-out. Profile of approximate square given by retaining two and three terms in the transformation function

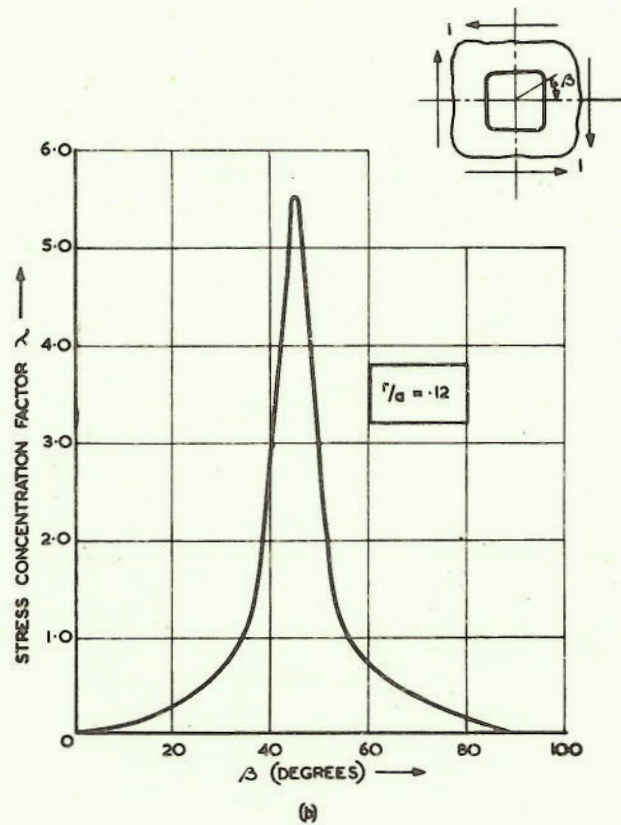
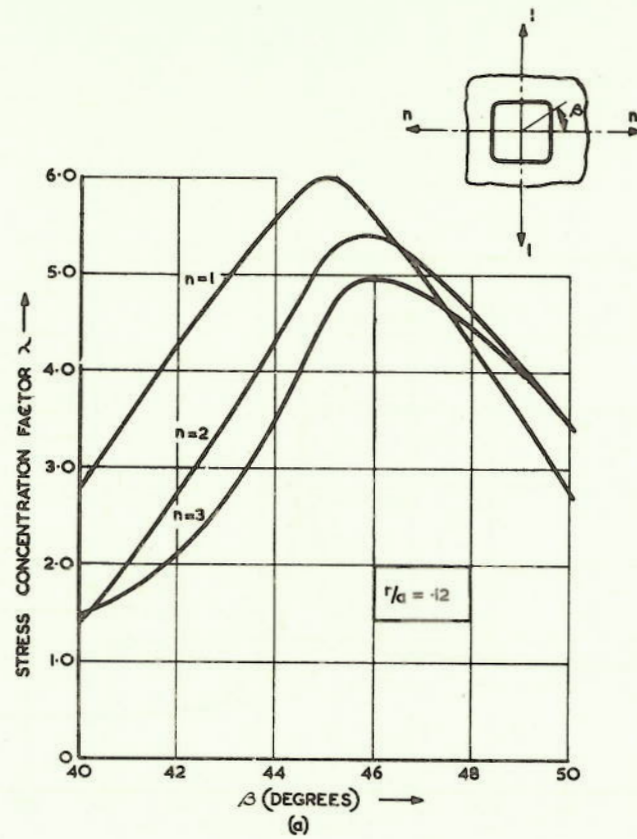


FIG. 7. Square cut-out ($\frac{r}{a} = .12$). Theoretical stress concentration factor when plate is subjected to biaxial tension or shear

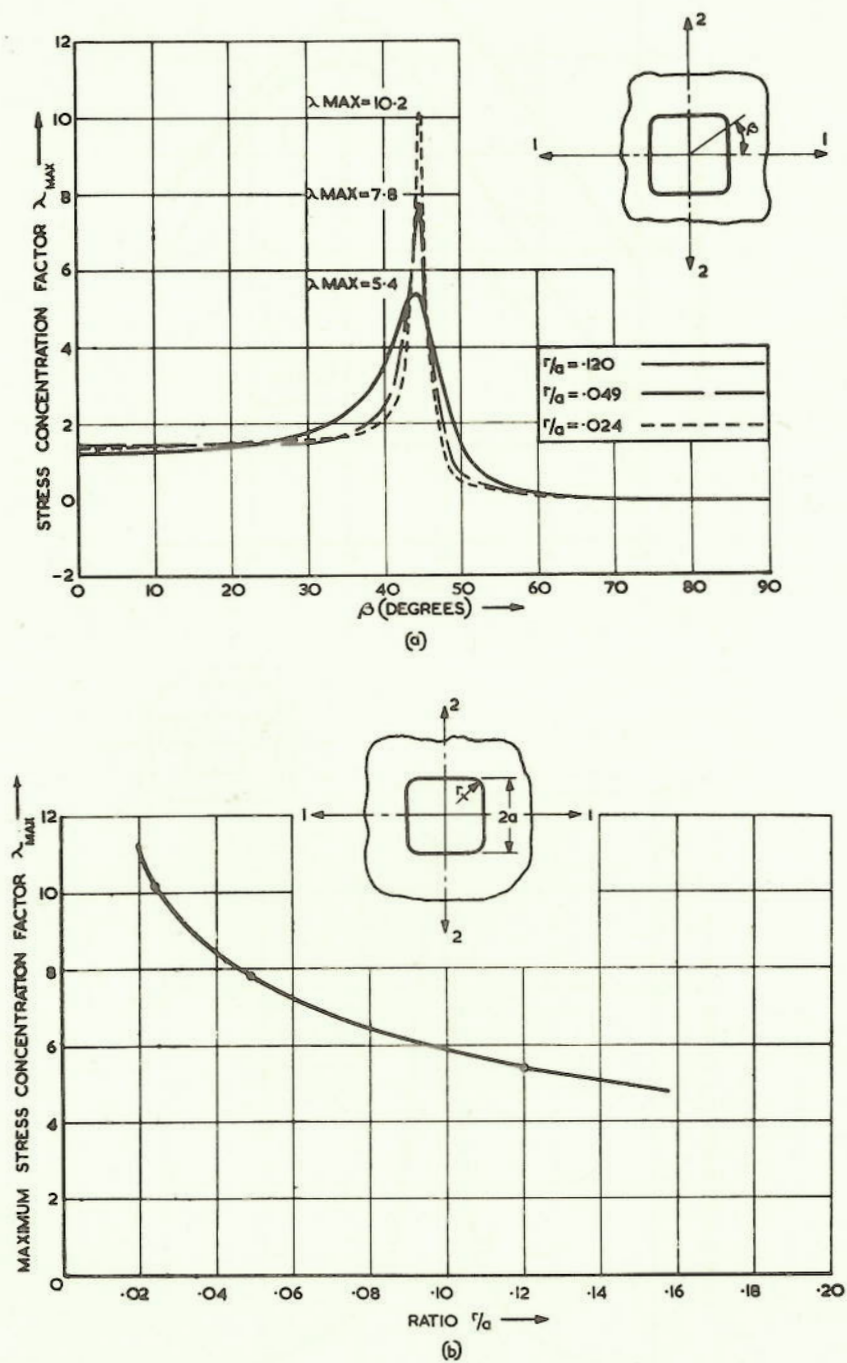


FIG. 8. Square cut-out. Theoretical stress concentration factor for various corner radii when plate is subjected to 2:1 biaxial tension

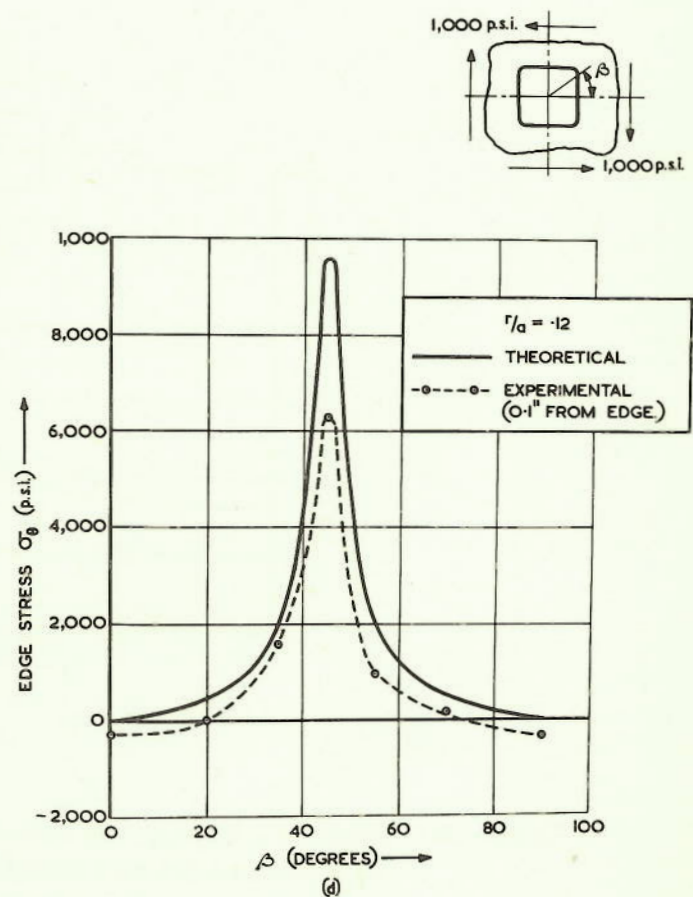
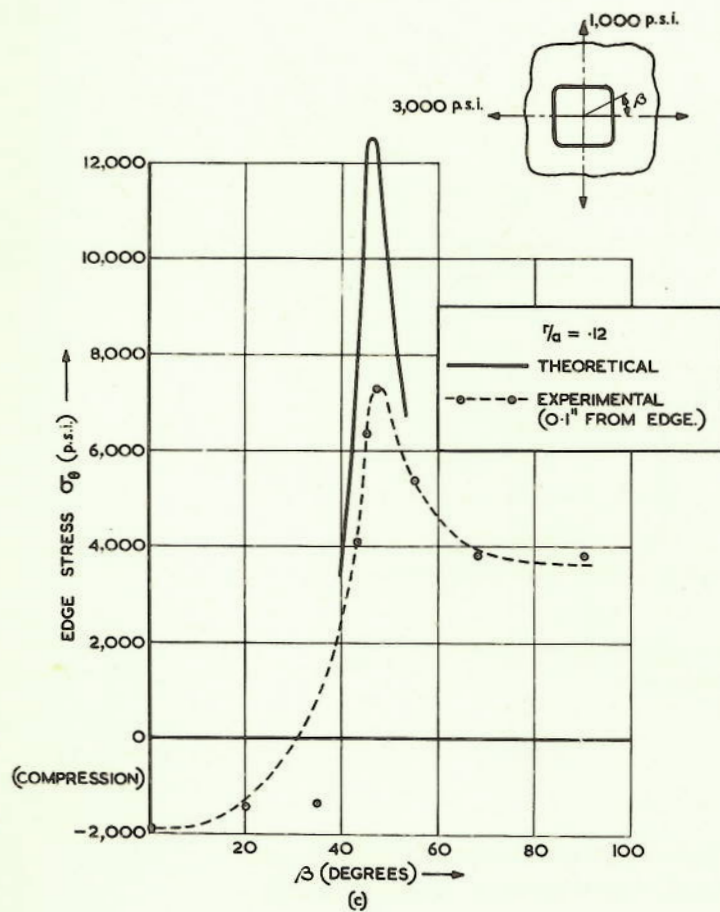
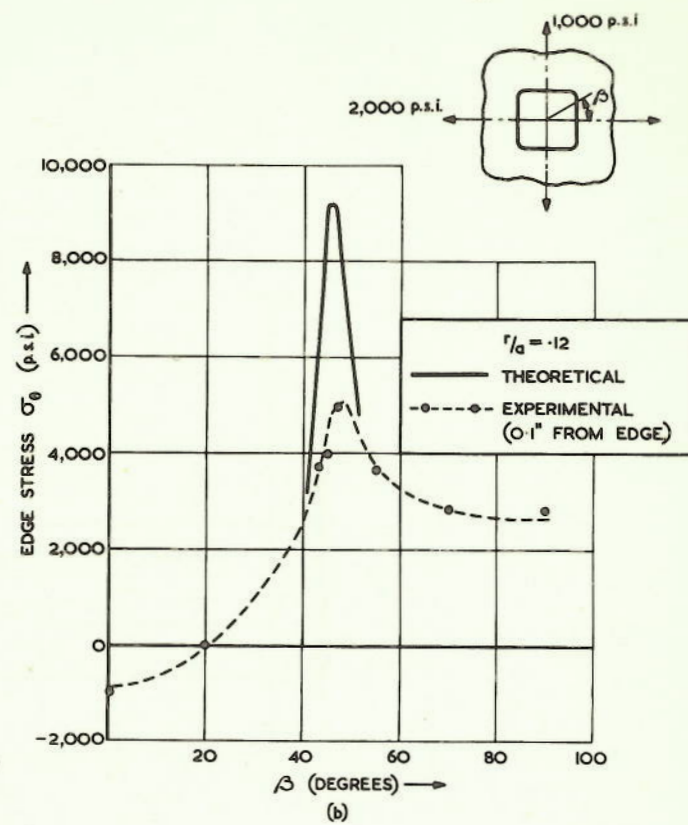
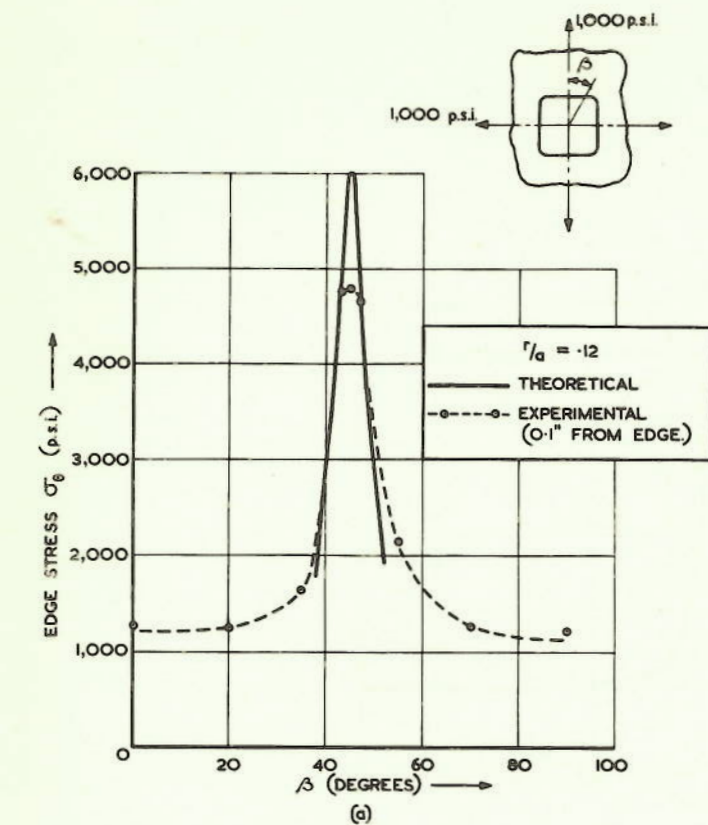


FIG. 9. Square cut-out ($\frac{r}{a} = .12$). A comparison between experimental and theoretical stress distributions when the plate is subjected to biaxial tension or shear

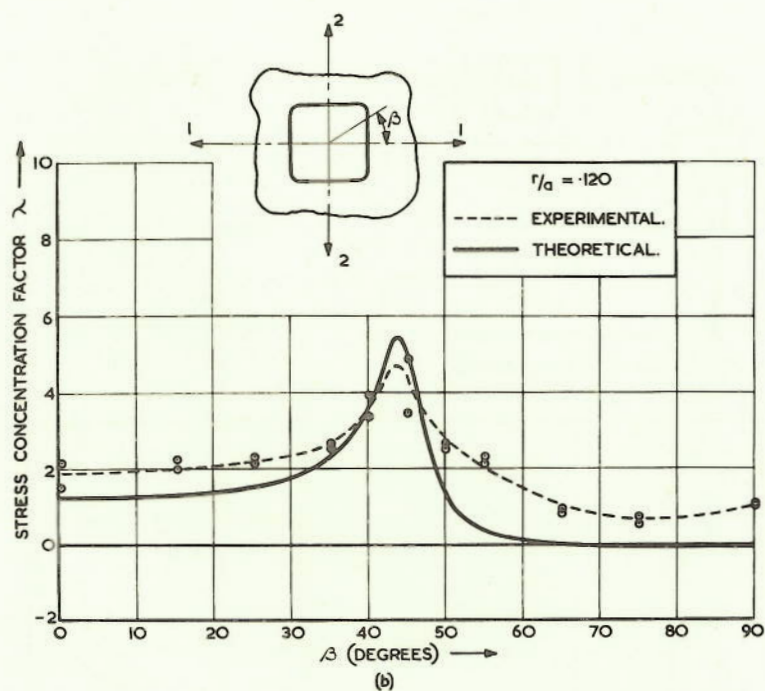
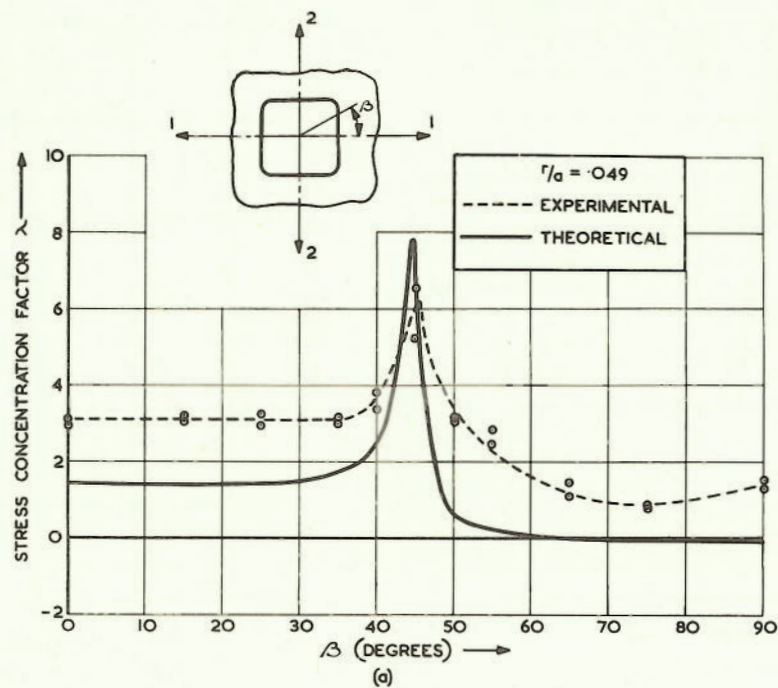


FIG. 10. Square cut-out. A comparison between experimental and theoretical stress distributions for various corner radii, when plate is subjected to 2:1 biaxial tension

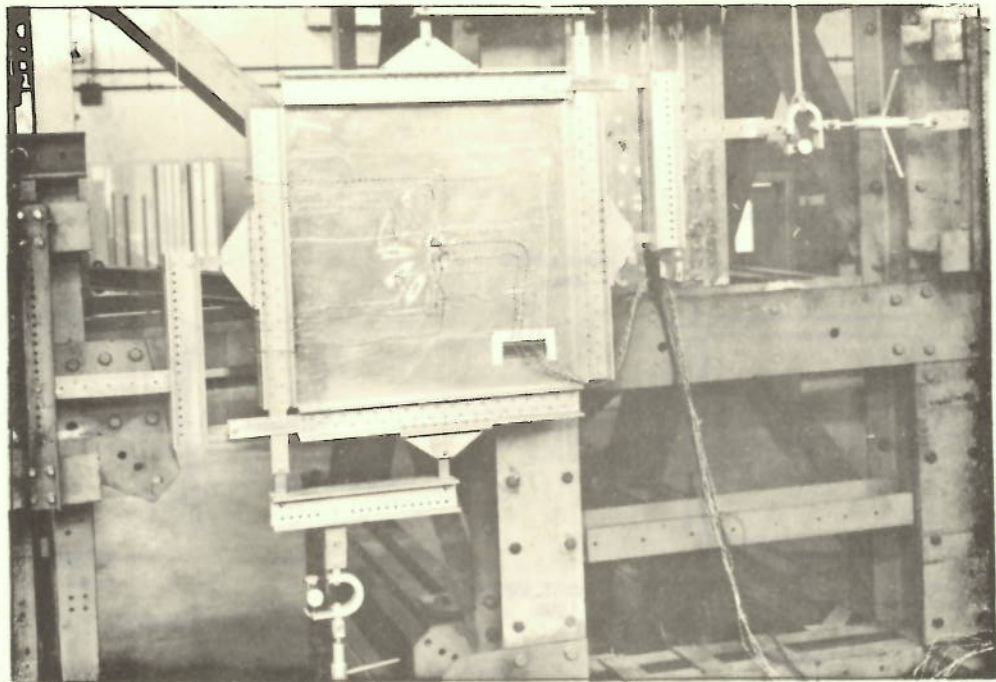


FIG. 11. PLANE LOADING FRAME SHOWING UNCUT PANEL

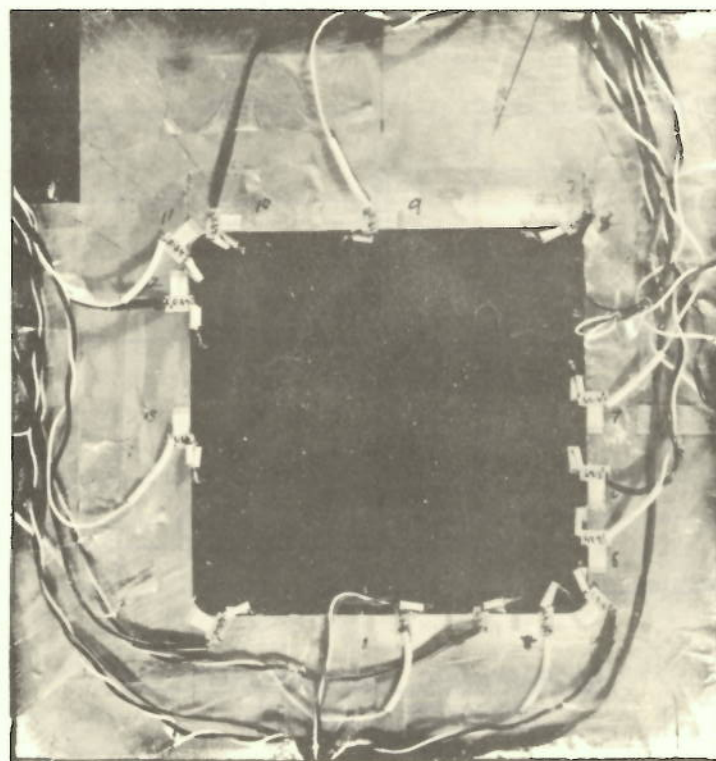
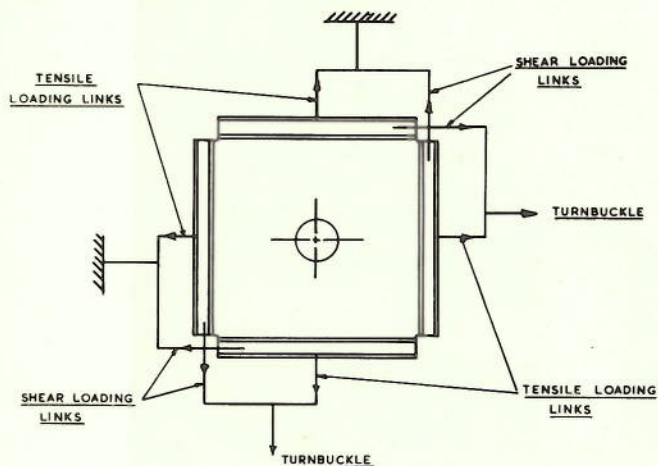
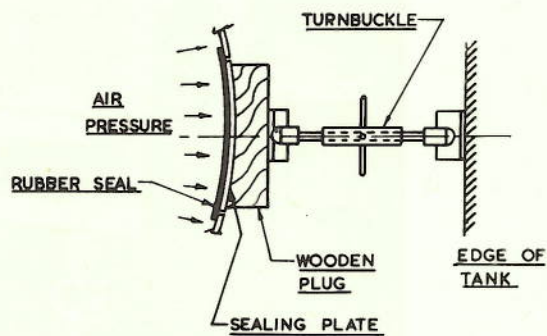


FIG. 12. TYPICAL CUT-OUT IN PANEL OF PLANE LOADING FRAME



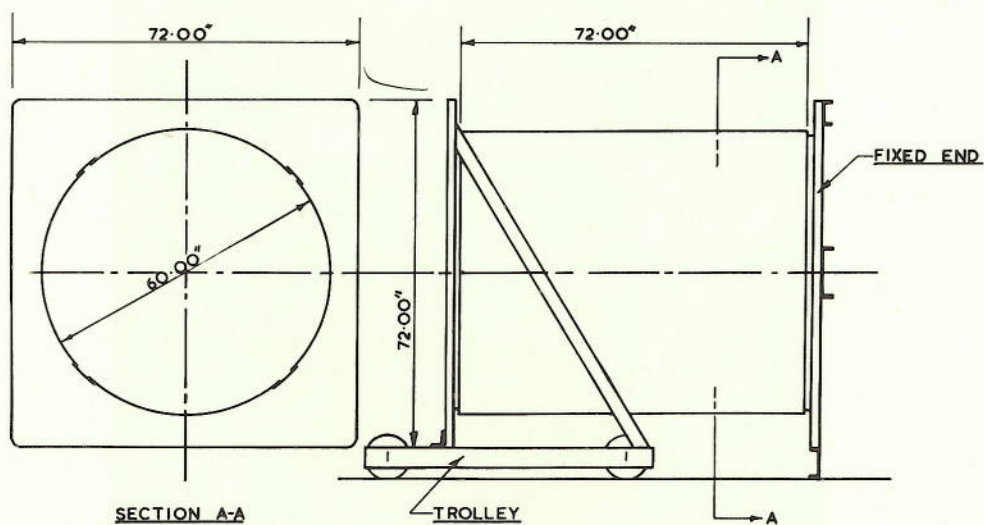
DIAGRAMMATIC ARRANGEMENT OF LOADING
FOR PANEL UNDER COMBINED BIAXIAL
TENSION AND SHEAR

FIG. 13.



METHOD OF SEALING CUT-OUT
IN PRESSURE CYLINDER

FIG. 15.



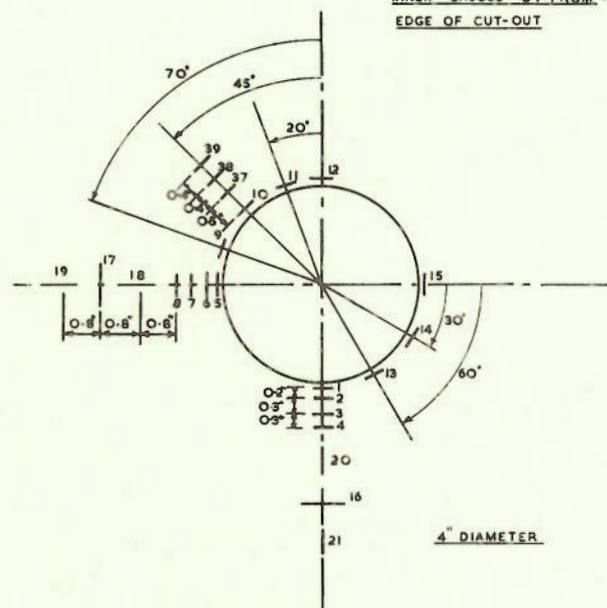
DIAGRAMMATIC ARRANGEMENT OF
PRESSURE CYLINDER

FIG. 14.

ALL GAUGES TINSLEY 5H TYPE
WITH EXCEPTION OF 16, 17, 18, 19, 20, 21

DISTANCES TO CENTRE LINE
OF GAUGES

INNER GAUGES 0.1" FROM
EDGE OF CUT-OUT



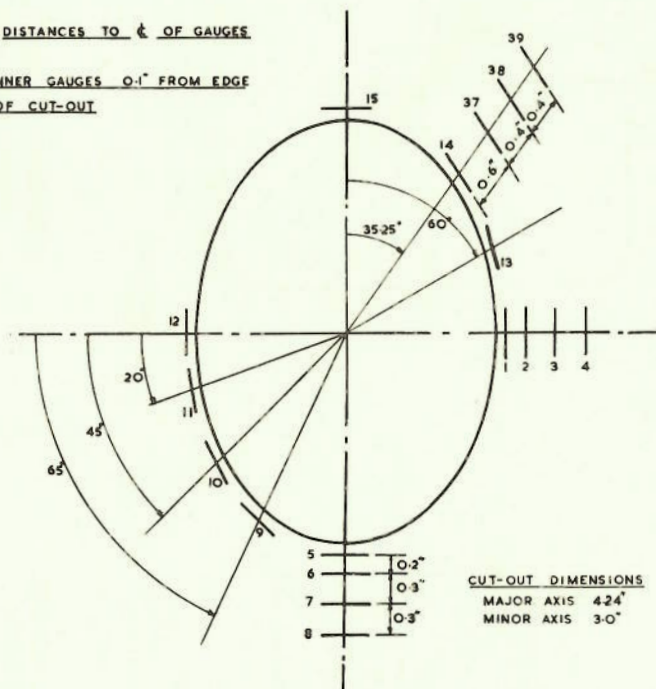
UNREINFORCED CIRCULAR CUT-OUT
STRAIN GAUGE POSITIONS
(PLANE LOADING FRAME)

FIG. 16.

ALL GAUGES TINSLEY 5H TYPE

DISTANCES TO $\frac{1}{4}$ OF GAUGES

INNER GAUGES 0.1" FROM EDGE
OF CUT-OUT

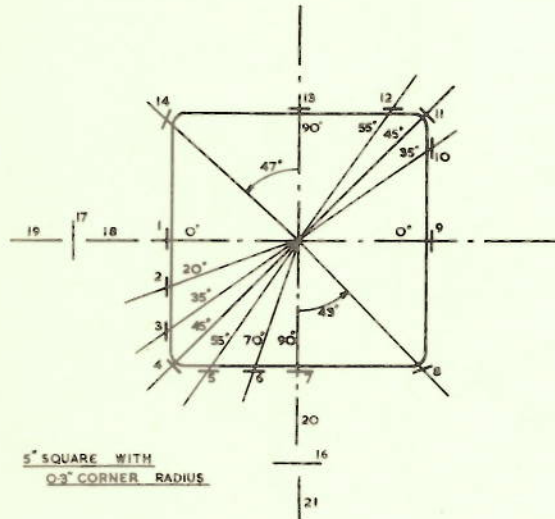


UNREINFORCED ELLIPTICAL CUT-OUT
STRAIN GAUGE POSITIONS
(PLANE LOADING FRAME)

FIG. 17.

TINSLEY 6H GAUGES

INNER GAUGES 0.1" FROM
EDGE OF CUT-OUT

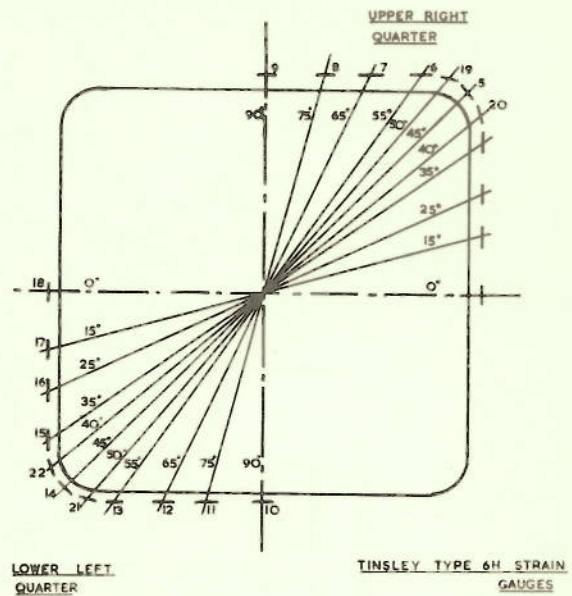


UNREINFORCED SQUARE CUT-OUT
STRAIN GAUGE POSITIONS
(PLANE LOADING FRAME)

FIG. 18.

OVERALL DIMENSION 10-40" SQUARE

STRAIN GAUGES APPROX 3/16" FROM
EDGE OF CUT-OUT



UNREINFORCED SQUARE CUT-OUT
STRAIN GAUGE POSITIONS
(60 IN. DIA. PRESSURE CYLINDER)

FIG. 19.

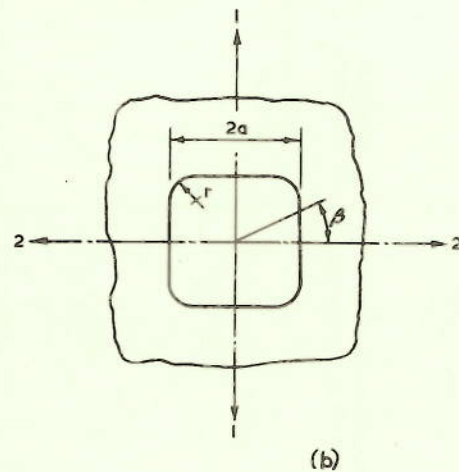
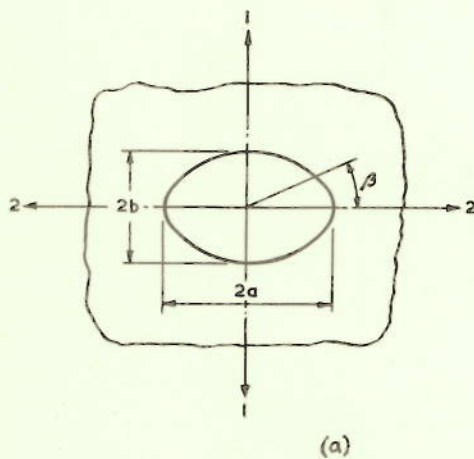


FIG. 20. CUT OUT DIMENSIONS AND LOADING
USED IN APPENDIX